

Chapter 5 Figures for Public Review

CHAPTER 5

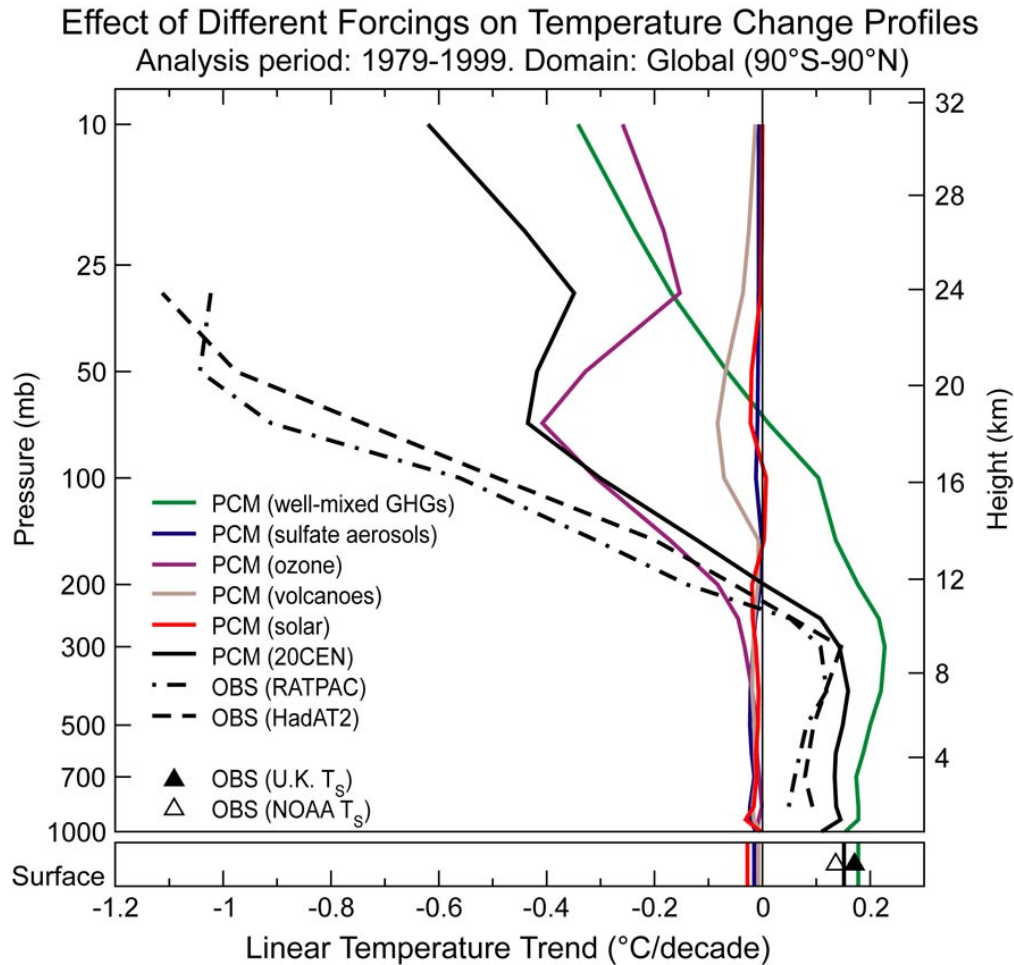


Figure 5.1: Vertical profiles of global-mean atmospheric temperature change over 1979 to 1999. Surface temperature changes are also shown. Results are from two different radiosonde data sets (HadAT2 and RATPAC; see Chapter 3) and from single forcing and combined forcing experiments performed with the Parallel Climate Model (PCM; Washington et al., 2000). PCM results for each forcing experiment are averages over four different realizations of that experiment. All trends were calculated with monthly mean anomaly data.

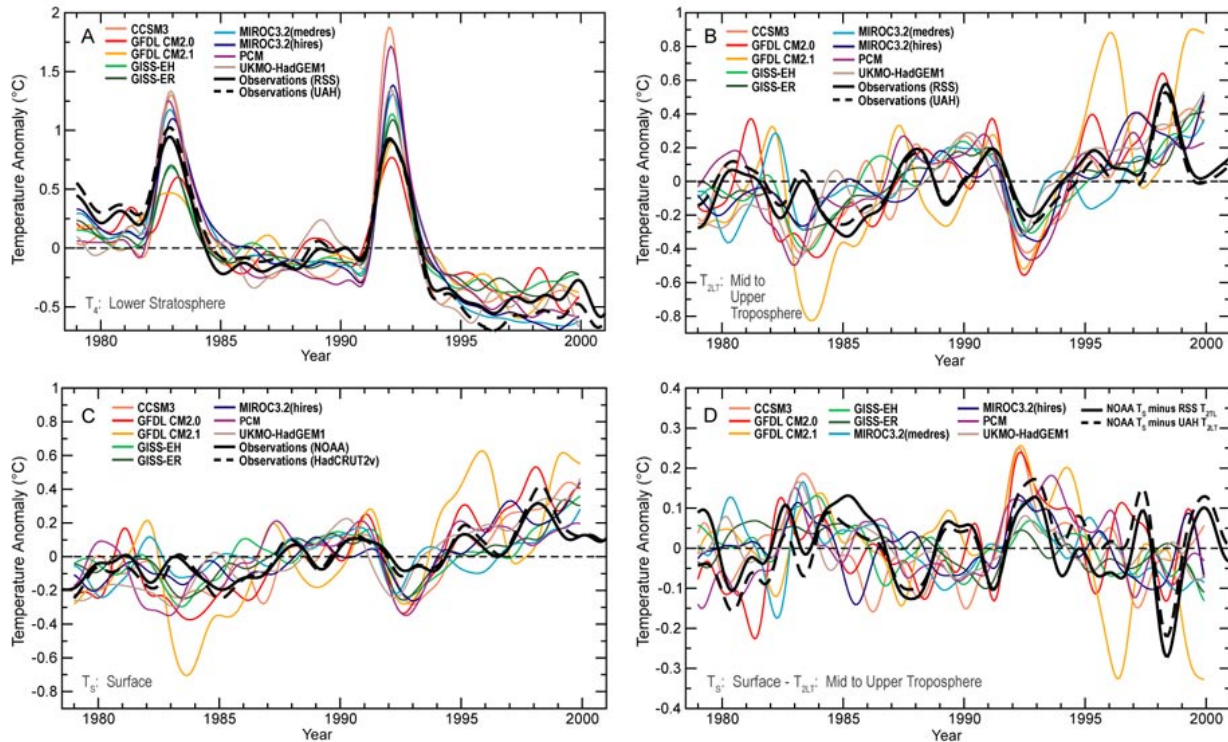


Figure 5.2A: Modeled and observed changes in global-mean monthly-mean lower stratospheric temperature (T_4). A simple weighting function approach (Box 2.2) was used to calculate a “synthetic” T_4 (equivalent to the MSU T_4 monitored by satellites) from model temperature data. Synthetic T_4 results are from “20CEN” experiments performed with nine different models (see Table 5.1). These models were chosen because they satisfy certain minimum requirements in terms of the forcings applied in the 20CEN run: all nine were driven by changes in well-mixed GHGs, sulfate aerosol direct effects, tropospheric and stratospheric ozone, volcanic aerosols, and solar irradiance (in addition to other forcings; see Table 5.2). Observed satellite-based estimates of T_4 changes were obtained from both RSS and UAH (see Chapter 3). All T_4 changes are expressed as departures from a 1979 to 1999 reference period average, and were smoothed with the same filter. To make it easier to compare the variability of T_4 in models with different ensemble sizes (see Table 5.1), only the first 20CEN realization is plotted from each model. This also facilitates comparisons of modeled and observed variability.

Figure 5.2B: As for Figure 5.2A, but for time series of global-mean, monthly-mean lower tropospheric temperature anomalies (T_{2LT}).

Figure 5.2C: As for Figure 5.2A, but for time series of global-mean, monthly-mean surface temperature anomalies (T_S).

Figure 5.2D: As for Figure 5.2A, but for time series of global-mean, monthly-mean temperature differences between the surface and T_{2LT} .

Modeled and Observed Temperature Trends in the Tropics (20°N-20°S)

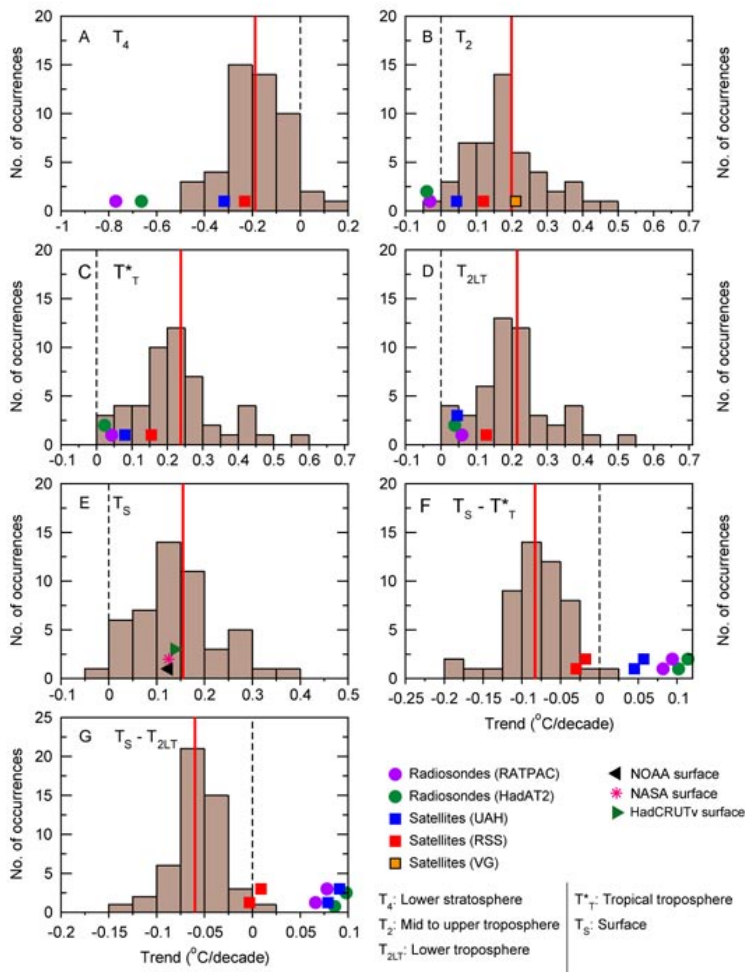


Figure 5.4: As for Figure 5.3, but for trends in the tropics (20°N-20°S).

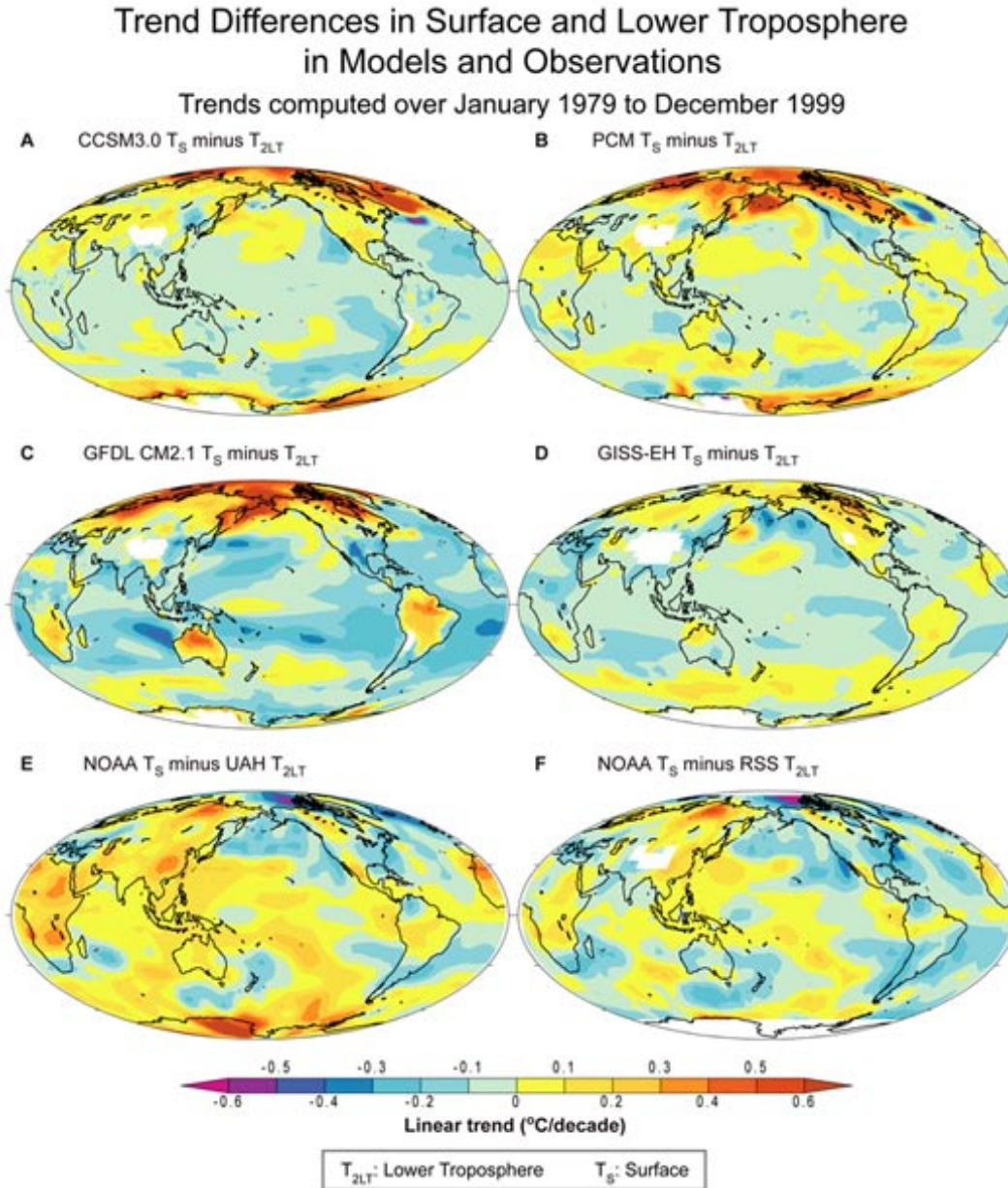


Figure 5.5: Modeled and observed maps of the differences between trends in TS and T2LT. All trends in TS and T2LT were calculated over the 252-month period from January 1979 to December 1999. Model results are ensemble means from 20CEN experiments performed with CCSM3.0 (**panel A**), PCM (**panel B**), GFDL CM2.1 (**panel C**), and GISS-EH (**panel D**). Observed results rely on NOAA TS trends and on two different satellite estimates of trends in T2LT, obtained from UAH (**panel E**) and RSS (**panel F**). White denotes high elevation areas where it is not meaningful to calculate synthetic T2LT (**panels A-D**). Note that RSS mask T2LT values in such regions, while UAH do not (**c.f. panels F, E**).

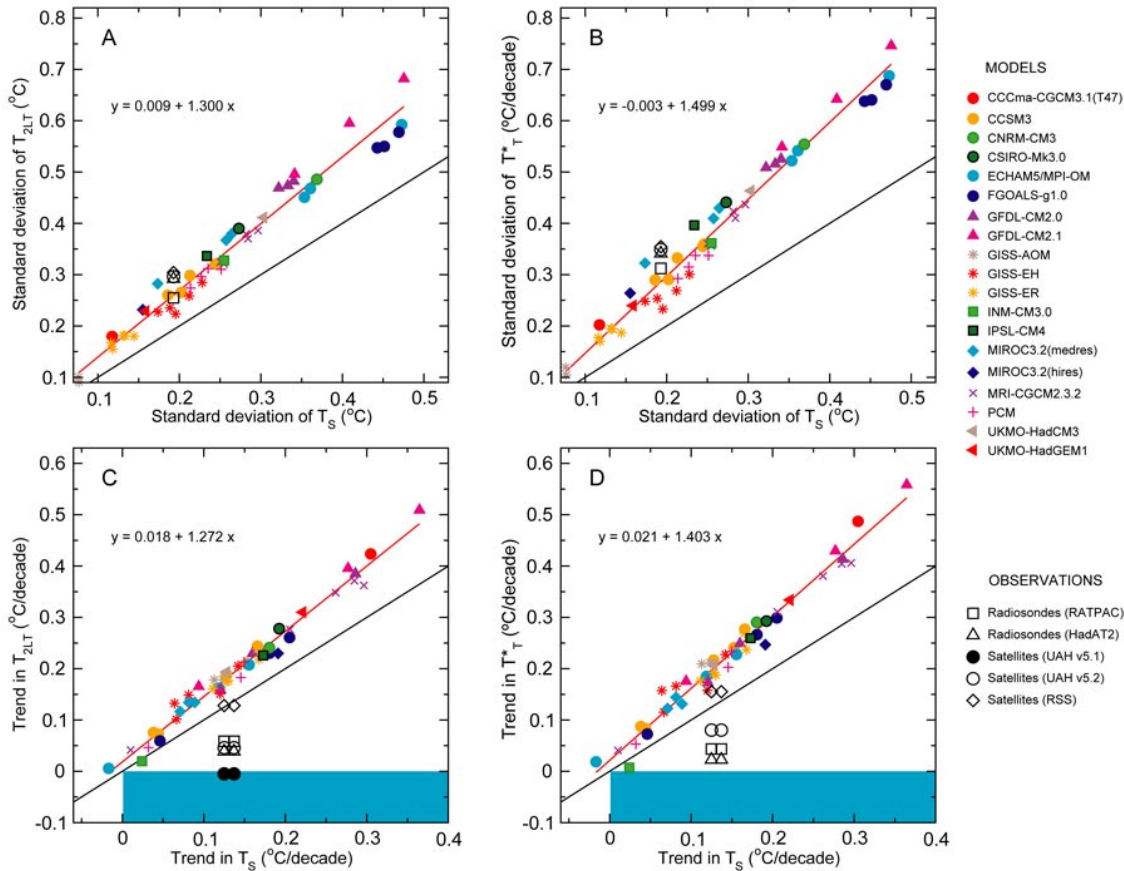


Figure 5.6: Scatter plots showing the relationships between tropical temperature changes at Earth’s surface and in two different layers of the troposphere. All results rely on temperature data that have been spatially-averaged over the deep tropics (20°N-20°S). Model data are from 49 realizations of 20CEN runs performed with 19 different models (Table 5.1). Observational results were taken from four different upper-air datasets (two from satellites, and two from radiosondes) and two different surface temperature datasets (see Chapter 3). The two upper panels provide information on the month-to-month variability in T_s and T_{2LT} (**panel A**) and in T_s and T^*T (**panel B**). The two bottom panels consider temperature changes on multi-decadal timescales, and show the trends (over 1979 to 1999) in T_s and T_{2LT} (**panel C**) and in T_s and T^*T (**panel D**). The red line in each panel is the regression line through the model points. Its slope provides information on the amplification of surface temperature variability and trends in the free troposphere. The black line in each panel is given for reference purposes, and has a slope of 1. Values above (below) the black lines indicate tropospheric amplification (damping) of surface temperature changes. There are two columns of observational results in C and D. These are based on the NOAA and HadCRUT2v T_s (0.12 and 0.14 $^{\circ}C/decade$, respectively). Note that panel C show results from published and recently-revised versions of the UAH T_{2LT} data (versions 5.1 and 5.2). Since the standard deviations calculated from NOAA and HadCRUT2v monthly T_s anomalies are very similar, observed results in A and B use NOAA standard deviations only. The blue shading in the bottom two panels defines the region of simultaneous surface warming and tropospheric cooling.

Zonal-Mean Atmospheric Temperature Change in Models and Data
Trends computed over January 1979 to December 1999

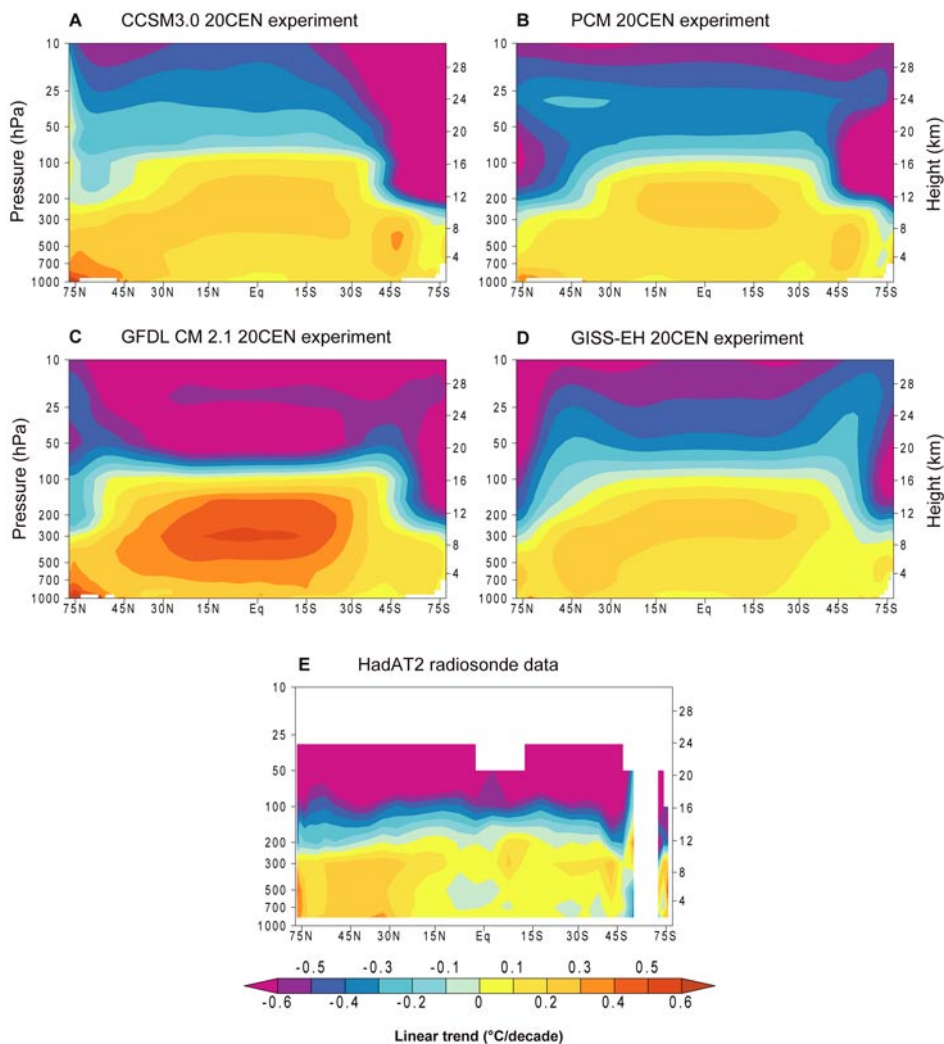


Figure 5.7: Zonal-mean patterns of atmospheric temperature change in “20CEN” experiments performed with four different climate models and in observational radiosonde data. Model results are for CCSM3.0 (**panel A**), PCM (**panel B**), GFDL CM 2.1 (**panel C**), and GISS-EH (**panel D**). The model experiments are ensemble means. There are differences between the sets of climate forcings that the four models used in their 20CEN runs (Table 5.3). Observed changes (**panel E**) were estimated with HadAT2 radiosonde data (Thorne et al., 2005, and Chapter 3). The HadAT2 temperature data do not extend above 30 hPa, and have inadequate coverage at high latitudes in the Southern Hemisphere. All temperature changes were calculated from monthly-mean data and are expressed as linear trends (in °C/decade) over 1979 to 1999.